

Scaling Laws for Adversarial Attacks on Language Model Activations

Stanislav Fort*

December 6, 2023

Abstract

We explore a class of adversarial attacks targeting the activations of language models. By manipulating a relatively small subset of model activations, a , we demonstrate the ability to control the exact prediction of a significant number (in some cases up to 1000) of subsequent tokens t . We empirically verify a scaling law where the maximum number of target tokens t_{\max} predicted depends linearly on the number of tokens a whose activations the attacker controls as $t_{\max} = \kappa a$, and find that the number of bits of control in the input space needed to control a single bit in the output space (that we call *attack resistance* χ) is remarkably constant between ≈ 16 and ≈ 25 over 2 orders of magnitude of model sizes for different language models. Compared to attacks on tokens, attacks on activations are predictably much stronger, however, we identify a surprising regularity where one bit of input steered either via activations or via tokens is able to exert control over a similar amount of output bits. This gives support for the hypothesis that adversarial attacks are a consequence of dimensionality mismatch between the input and output spaces. A practical implication of the ease of attacking language model activations instead of tokens is for multi-modal and selected retrieval models, where additional data sources are added as activations directly, sidestepping the tokenized input. This opens up a new, broad attack surface. By using language models as a controllable test-bed to study adversarial attacks, we were able to experiment with input-output dimensions that are inaccessible in computer vision, especially where the output dimension dominates.

Two sentence summary: *Manipulating just one token’s activations in a language model can precisely dictate the subsequent generation of up to $\mathcal{O}(100)$ tokens. We further demonstrate a linear scaling of this control effect across various model sizes, and remarkably, the ratio of input control to output influence remains consistent, underscoring a fundamental dimensional aspect of model adversarial vulnerability.*

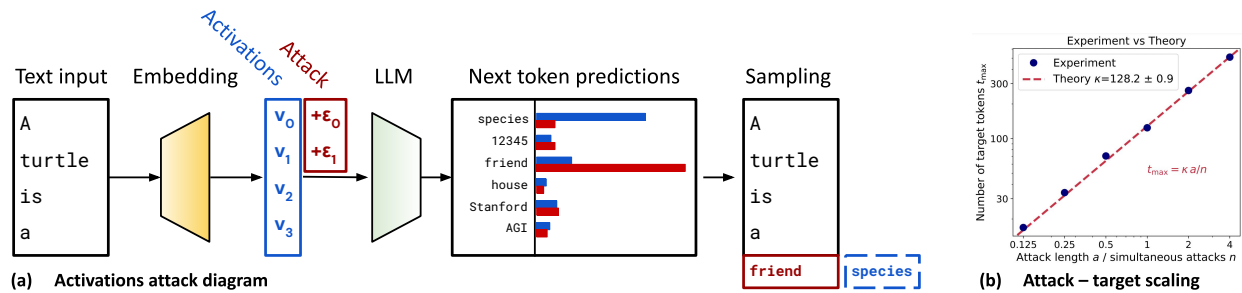


Figure 1: **(Left panel)** A diagram showing an attack on the activations (blue vectors) of a language model that leads to the change of the predicted next token from *species* to *friend*. **(Right panel)** The maximum number of tokens whose values can be set precisely, t_{\max} , scales linearly with the number of attack tokens a .

*Now at Google DeepMind. Work done while independent.

1 Introduction

Adversarial attacks pose a major challenge for deep neural networks, including state-of-the-art vision and language models. Small, targeted perturbations to the model input can have very large effects on the model outputs and behaviors. This raises concerns around model security, safety and reliability, which are increasingly practically relevant as machine learning systems get deployed in high-stakes domains such as medicine, self-driving, and complex decision making. While most work has focused on attacking image classifiers, where adversarial examples were first identified (Szegedy et al., 2013), large language models (LLMs) both 1) provide a natural, controllable test-bed for studying adversarial attacks more systematically and in otherwise inaccessible regimes, and 2) are of a great importance on their own, since they are increasingly becoming a backbone of many advanced AI applications.

An adversarial attack on an image classifier is a small, targeted perturbation added to its continuous input (e.g. an image) that results in a dramatic change of the resulting classification decision from one class to another, chosen by the attacker. Working with language models, we immediately face two core differences: their input is a series of discrete tokens, not a continuous signal, and the model is often used in an autoregressive way (popularly referred to as "generative") to generate a continuation of a text, rather than classification. In this paper, we side step the discrete input issue by working with the continuous model activations (sometimes referred to as the residual stream (Elhage et al., 2021)) that the discrete tokens get translated to by the embedding layer at the very beginning of the model. We resolve the second issue by viewing a language model as a classifier from the continuous activations (coming from input tokens) to a discrete set of t -token continuations that are drawn from V^t possibilities (V being the vocabulary size of the model). We compare these *activation attacks* to *token substitution attacks* as well.

We hypothesize that the mismatch between the dimensions of the input space (that the attacker can control) and the output space is a key reason for adversarial susceptibility of image classifiers, concretely the much larger input dimension over the output one. A similar argument can be traced through literature (Goodfellow et al., 2015; Abadi et al., 2016; Ilyas et al., 2019). Beyond immediate practical usefulness (argued later), directly manipulating the floating point activation vectors within a language model rather than substituting input tokens makes our situation exactly analogous to image classification, with a key difference that we can now control both the input and output space dimension easily. Concretely, we change the activations of the first a tokens of the input out of a context of length s ($a < s$) in order to precisely control the model output for the following t tokens down to the specific tokens being produced (sampled by argmax). By varying a , we exponentially control the input space dimension, while varying t gives us an exponential control over the output space dimension. Doing this, we identify an approximate empirical scaling law connecting the attack length a , target length t , and the dimension of the activations d , which holds over two orders of magnitude in parameter count and different model families, and that is supported by theory.

Does a significant vulnerability to activation attacks pose a practical vulnerability given that a typical level of access to a large language model stays at the level of input tokens (especially for commercial models)? While token access is standard, there are at least two very prominent cases where an attacker might in fact access and control the activations directly:

1. **Retrieval:** Borgeaud et al. (2022) uses a database of chunks of documents that are on the fly retrieved and used by a language model. Instead of injecting the retrieved pieces of text directly as *tokens*, a common strategy is to encode and concatenate them with the prompt activations directly, skipping the token stage altogether. This gives a direct access to the activations to whoever controls the retrieval pipeline. Given how few activation dimensions we can use to generate concrete lengthy outputs (e.g. 100 exact tokens predicted from a single token-worth of activations attacked), this gives the attacker an unparalleled level of control over the LLM.
2. **Multi-modal models:** Alayrac et al. (2022) insert embedded images as activations in between text token activations to allow for a text-image multi-modal model. Similarly to the retrieval case, this allows an attacker to modify the activations directly. It is likely that similar approaches are used by other vision-LMs as well as LMs enhanced with other non-text modalities, posing a major threat.

Related work. Understanding a full LLM-based system instead of just analyzing the main model has been highlighted in [DeBenedetti et al. \(2023\)](#) as very relevant to security, as the add-ons on top of the main LLM open additional attack surfaces. Similar issues have been highlighted among open questions and problems in reinforcement learning from human feedback (RLHF, [Bai et al. \(2022\)](#)) ([Casper et al., 2023](#)). Modifying model activations directly was also done in [Zou et al. \(2023a\)](#).

Scaling laws for language model performance, as a function of the parameter count and the amount of data, have been identified in [Kaplan et al. \(2020\)](#), refined in [Hoffmann et al. \(2022\)](#) and worked out for sparsely-connected models in [Frantar et al. \(2023\)](#). Similar empirical dependencies are also frequent in machine learning beyond performance prediction, e.g. the dependence between classification accuracy and near out-of-distribution robustness ([Fort et al., 2021](#)). Scaling laws have been identified in biological neural networks, for example between the number of neurons and the mass of the brain in mammals ([Herculano-Houzel, 2012](#)), and birds ([Kabadayi et al., 2016](#)), showing that performance scales with the log of the number of pallial or cortical neurons.

Using activation additions ([Turner et al., 2023](#)) shows some level of control over model outputs. A broad exploration and literature on model jail-breaking can also be seen in the light of adversarial attacks. [Zou et al. \(2023b\)](#) uses a mixture of greedy and gradient-based methods to find token suffixes that "jail-break" LLMs. [Wang et al. \(2023\)](#) claims that larger models are easier to jailbreak as a consequence of being better at following instructions. Attacks on large vision models, such as CLIP ([Radford et al., 2021](#)) are discussed in e.g. [Fort \(2021a,b\)](#).

Our contributions in this paper are as follows:

1. Scaling laws for adversarial attacks to LLM activations (or residual streams): We theoretically predict a simple scaling "law" that relates the maximum achievable number of output tokens that an attacker can control precisely, t_{\max} , to the number of tokens, a , whose activations (residual streams) they control. We also connect this to the number of simultaneous sequences and the number, n , of targets they can attack with the same activation perturbation at the same time (similar to multi-attacks in [Fort \(2023\)](#)) and the fraction of activation dimensions they are using, f , as

$$t_{\max} = \kappa f \frac{a}{n}, \tag{1}$$

where κ is a model-specific constant that we call an *attack multiplier* and that we measure for models from 33M to 2.8B parameters. Details are shown in [Figure 7](#) and [Table 1](#).

2. The constant κ , being the number of target tokens a single attack token worth of activations can control in detail, scales empirically surprisingly linearly with the activation (residual stream) dimension d , with d/κ being measured between 16 and 25 for a model family, suggesting that each input dimension the attacker controls effects approximately the same number of output dimension. We convert this to *attack resistance* χ that characterizes how many bits in the input space the attacker needs to control to determine a single bit in the output space. This supports the hypothesis of adversarial vulnerability as a dimension mismatch issue.
3. A comparison of greedy substitution attacks on input tokens and activation attacks. For our 70M model, we show that we need approximately 8 attack tokens to affect a single output token via token substitution, while attacking activations requires $\approx 1/24$ of a token. Comparing the dimensionalities of the input space for the two attacks, we show the attack strength is within a factor of 2 of each other for both methods, further supporting the dimension hypothesis. Details in [Figure 9](#).
4. Exploring the effect of separating the attack tokens from the target tokens by an intermediate context. The attack strength does not seem to decrease for up to 100 tokens of separation and decreases only logarithmically with context length after. Even at $\mathcal{O}(1000)$ tokens of separation, the activations of the very first token can determine ≈ 8 tokens at the very end (for our 70M model experiment, see [Figure 8](#)).

2 Theory

2.1 Problem setup

Given an input string that gets tokenized into a series of s integer-valued tokens S (each drawn from a vocabulary of size V as $S_i \in \{0, 1, \dots, V - 1\}$), a language model f can be viewed as a classifier predicting the probabilities of the next-token continuation of that sequence over the vocabulary V . Were we to append the predicted token to the input sequence, we would be running the language model in its typical, autoregressive manner. Given this new input sequence, we could get the next token after, and repeat the process for as long as we need to.

Let’s consider predicting a t -token sequence that would follow the input context. There are V^t such possible outputs. This process is now mapping an s -token input sequence, for which there are V^s many combinations, into its t -token continuation, for which there are V^t combinations. Out of the s input tokens, we could choose a subset of $a \leq t$ that would be the *attack* tokens the attacker can control. In this setup, we have a controllable classification experiment where the dimension of the input space a (that the attacker controls), and the dimension of the target space, t , that they wish to determine the outputs in, are experimental dials that we can set and control explicitly.

2.2 Attacking activation vectors

To match the situation to the usual classification setup, we need a continuous input space. Instead of studying the behavior of the full language model mapping s (or a) discrete tokens into probabilities of t -token sequences, we can first turn the input sequence S into activation vectors, each of dimension d , (sometimes referred to as the *residual stream* (Henighan et al., 2023)) as $f_{\text{before}}(S \in \{0, 1, \dots, V - 1\}^s) = v \in \mathbb{R}^{s \times d}$, and then propagate these activations through the rest of the network as $f_{\text{after}}(v)$.

The goal of the attacker is to come up with a perturbation P to the first a token activations (an arbitrary choice) within the vector v such that the argmax autoregressive sampling from the model would yield the target sequence T as the continuation of the input sequence S . Practically, this means that we can imagine computing the activations v from the input sequence S by the embedding layer, adding the perturbation P to it, and passing it on through the rest of the model to get the next token logits. If the attack is successful, then $\text{argmax} f_{\text{after}}(v + P) = T_0$. For the j^{th} target token, we get the activations of the input string S concatenated with $(j - 1)$ tokens of the target sequence, $f_{\text{before}}(S + T[:j])$, add the perturbation P (that does not affect the activations of more than the first a tokens $a \leq |S| \leq |S + T[:j]|$), and for a successful attack obtain the prediction of the next target token as $\text{argmax} f_{\text{after}}(f_{\text{before}}(S + T[:j]) + P) = T_j$. What is described here is a success condition for the attack P towards the target sequence T rather than a process to actually compute it practically, which is detailed in Section 3.3.

2.3 Input and output space dimensions

In a typical image classification setting, the number of classes is low, and consequently so is the dimension of the output space compared to the input space. For example, CIFAR-10 and CIFAR-100 have 10 and 100 classes respectively (Krizhevsky et al., a,b) (with $32 \times 32 \times 3 = 3072$ -dimensional images), ImageNet has 1,000 classes (Deng et al., 2009), and ImageNet-21k 21,000 ($\log_2(21,000) \approx 14$) (Ridnik et al., 2021) with $224 \times 224 \times 3 = 150,528$ -dimensional images.

In comparison, predicting a single token output for a language model already gives us $V \approx 50,000$ classes (for the tokenizer used in our models, typical numbers are between 10,000, and several 100,000s), and moving to t -token continuations gives us an exponential control over the number of classes. For this

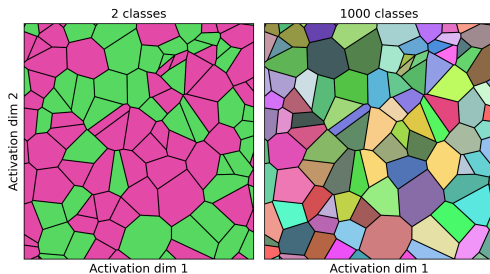


Figure 2: The difference between having fewer or the same number of classes than attack dimensions (on the left) and more classes than dimensions (on the right). In the former case, neighboring cells of all different classes are common, allowing for easy to find adversarial attacks.

reason, using a language model as a controllable test-bed for studying adversarial examples is very useful. Firstly, it allows us to control the output space dimension, and secondly, it opens up output spaces of much higher dimensions than would be accessible in standard computer vision problems. In our experiments, we study target sequences of up to $t \approx 1000$ tokens, giving us $V^t \approx 2^{16000}$ options or *effective* classes in our “classification” problem. For our LLM experiments, we actually get to realistic regimes in which the dimension of the space of inputs the attacker controls is much lower than the dimension of the space of outputs. As illustrated in Figure 2, this is a prerequisite for class regions of different classes in the space of inputs not neighboring each other by default. The exact limit would be the one where the input and output space dimensions were equal, but the higher the output dimension over the input dimensions, the easier it is to guarantee that adversarial examples will generically not be available in the neighborhood of a typical input point.

The attacker controls a part of the activation vector v with a perturbation P that has non-zero elements in the first a token activations. a determines the expressivity of the attack and therefore the attack strength. Unlike an attack on the discrete input tokens, each drawn from V possibilities, controlling a d -dimensional vector of floating point numbers per token, each number of 16 bits itself, offers a vastly larger dimensionality to the attacker (although of course the model might not be utilizing the full 16 bits after training, signs of which we see in Section 4). There are 2^{16^d} possible single token activation values, compared to just V for tokens. For example, for $d = 512$ and $V = 50000$ (typical numbers), $2^{16^d} = 2^{2048}$, while $V \approx 2^{16}$.

2.4 Scaling laws

The core hypothesis is that the ability to carry a successful adversarial attack depends on the ratio between the dimensions of the input and output spaces. The success of attacking a language model by controlling the activation vectors of the first a tokens, hoping to force it to predict a specific t -token continuation after the context, should therefore involve a linear dependence between the two. Let us imagine a t_{\max} , the maximum length of a target sequence the attacker can make the model predict with a attack tokens of activations. The hypothesized dependence is $t_{\max} \propto a$, or

$$t_{\max} = \kappa a, \tag{2}$$

where the specific scaling constant κ is the *attack multiplier*, and tells us how many tokens on the output can a single token worth of activations on the input control. We can test the scaling law in Eq. 2 by observing if the maximum attack length t scales linearly with the attack length a . The specific attack strength κ is empirically measured and specific to each model.

If we were to use only a fraction f of the activation vector dimensions in the a attack tokens, the effective dimension the attacker controls would equivalently decrease by a factor of f . Therefore the revised scaling law would be $t_{\max} = \kappa f a$. We verify that the effect of the fraction of dimensions on the successful target length is the same as varying the attack length a .

$$t_{\max} = \kappa f a \tag{3}$$

In Fort (2023), the authors develop a single perturbation P called a *multi-attack* that is able to change the classification of n different images to n arbitrary classes chosen by the attacker. This effectively increases the dimension of the output space by a factor of n , while keeping the attack dimension of P constant, which is a useful fact for us. We run experiments in this setup as well, where we want a single activation perturbation P to continue a context S_1 by a target sequence T_1 , S_2 by T_2 , and so on all the way to S_n to T_n . The dimension of the output space increases by a factor n , and therefore the maximum target length t_{\max} now scales as $t_{\max} n = \kappa f a$. The revised scaling law is therefore

$$t_{\max} = \kappa f a / n. \tag{4}$$

The attack strength κ is model specific and empirically determined. However, our geometric theory suggests that it should be linearly dependent on the dimension of the activations of the model. Let us consider a simple model where χ bits of control on the input are needed to determine a single bit on the output, and

let us call χ the *attack resistance*. For a vocabulary of size V , each output token is specified by $\log_2 V$ bits. A single token has an activation vector specified by d p -bit precision floating point numbers. There are therefore dp bits the attacker controls by getting a hold of a single token of activations. The attack strength κ , which is the number of target tokens the attacker can control with a single token of an attack activation, should therefore be $\chi\kappa\log_2 V = dp$. We assume χ to be constant between models (although adversarial training probably changes it), and therefore our theory predicts that

$$\kappa = \frac{dp}{\chi \log_2 V}, \quad (5)$$

for a fixed attack resistance χ . For a fixed numerical precision and vocabulary size, the resulting scaling is $\kappa \propto d$, i.e. the attack strength is directly proportional to the dimension of the activation vector (also called the residual stream), and we observe this empirically in e.g. Table 1. Having obtained empirically measured values of κ , we can estimate the attack resistance χ , which we do in Section 4. In the simplest setting, we would expect $\chi = 1$, which would mean that a single dimension of the input controls a single dimension of the output. The specifics of the way input and output spaces map to each other are likely complex and the reason for why $\chi > 1$.

2.5 Comparison to token-level substitution attacks

As a comparison, we tried looking for token substitution attacks as well, which are significantly less expressive. For those, the attacker can change the first a integer-valued tokens on the input (instead of their high-dimensional activations; we illustrate this comparison in Figure 3; the geometric of the input manifolds is discussed in e.g. (Fort et al., 2022)), trying to make the model produce the attacker-specified t -token continuation as before. If the geometric theory from Section 2 holds, the prediction would be that the attack strength would go down by a factor proportional to the reduction in the dimension of the input space the attacker controls. Going from adp bits of control to $a\log_2 V$ bits corresponds to a $dp/\log_2 V$ reduction, which means that the attack multiplier κ_{token} for the token substitution method is predicted to be related to the activation attack strength κ as

$$\kappa_{\text{token}} = \kappa \frac{\log_2 V}{dp}. \quad (6)$$

For $d = 512$ and $V = 50000$, the $\frac{\log_2 V}{dp} \approx 2 \times 10^{-3}$. Our results are shown in Section 4, specifically in Table 2. In addition, it is very likely that the full 16 bits of the activation dimensions are not used, and that instead we should be using a $p_{\text{effective}} < p$.

3 Method

3.1 Problem setup

A language model takes a sequence of s integer-valued tokens $S = [S_1, S_2, \dots, S_s]$, each drawn from a vocabulary of size V , $S_i \in \{0, 1, \dots, V - 1\}$, and outputs the logits z over the vocabulary for the next-word prediction $z \in \mathbb{R}^V$. These are the unscaled probabilities that turn into probabilities as $p = \text{softmax}(z)$ over the vocabulary dimension. As described in Section 2, we primarily work with attacking the continuous model activations rather than the integer-valued tokens themselves.

The tokens S are first passed through the embedding layer of the language model, producing a vector v of d dimensions per token, $v = f_{\text{before}}(S)$. (These are the activations that the attacker can modify by adding a perturbation vector P .) After that, the activations pass through the rest of the language model, as $f_{\text{after}}(v) = z$, to obtain the logits for the next-token prediction. The full language model mapping tokens to

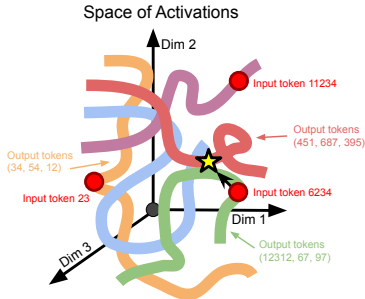


Figure 3: An illustration of the space of activations being partitioned into regions that get mapped to different t -token output sequences \approx our output classes.

logits would be $f_{\text{after}}(f_{\text{before}}(S)) = z$, we just decided to split the full function $f : S \rightarrow z$ into the two parts, exposing the activations for an explicit manipulation. The split need not happen after the embedding layer, but rather after L transformer layers of the model itself. While we ran exploratory experiments with splitting later in the model, we nonetheless performed all our detailed experiments with activations directly after the embedding layer.

3.2 An attack on activations

The attacker controls the activation perturbation P that gets added to the vector v in order to modify the next-token logits towards the token desired by the attacker. The modified logits are

$$z' = f_{\text{after}}(f_{\text{before}}(S) + P), \tag{7}$$

where P , the attack vector, is of the shape $P \in \mathbb{R}^{s \times d}$ (the same as v), however, we allow the attacker to control only the activations of the first $a \leq s$ tokens. This is an arbitrary choice and other variants could be experimented with. The attack comprises the first a tokens, leaving the remaining $s - a$ tokens separating the attack from its target. We experiment with the effect of this separation in Section 4.4.

While the attacker controls the activations of the first a tokens in the context, the model as described so far deals with affecting the prediction of the next token immediately after the s tokens in the context. As discussed in Section 2, we want to predict t -token continuations instead.

3.3 Loss evaluation and optimization

To evaluate the loss $\mathcal{L}(S, T, P)$ of the attack P on the context S towards the target multi-token prediction T , we compute the standard language modeling cross-entropy loss, with the slight modification of adding the perturbation vector P to the activations after the embedding layer. The algorithm is shown in Figure 8. To find an adversarial attack, we first choose a fixed, randomly sampled context of size S , define the attack

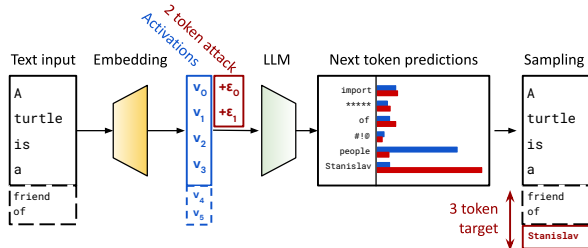


Figure 4: A diagram showing the $t = 3$ multi-token target prediction after an attack on $a = 2$ token activations.

Algorithm 1 Computing loss for an activation attack P towards a t -token target sequence

- 1: **Given** activation dimension d , tokens of context S of length $s = |S|$, attack length a ($a \leq s$), target tokens T of length t , and an attack vector $P \in \mathbb{R}^{a \times d}$
 - 2: Compute the activations of the context followed by the target $v = f_{\text{before}}(S + T) \in \mathbb{R}^{(s+t) \times d}$
 - 3: Add the perturbation vector to the first a tokens of v as $v' = v$, $v'[:a] += P$ {This is the attack}
 - 4: **for** $i = 0$ **to** $t - 1$ **do**
 - 5: Predict logits after the $s + i$ tokens of the context and target $z_i = f_{\text{after}}(v'[:s + i])$
 - 6: Compute the cross-entropy loss ℓ_i between these logits z_i and the target token $T[i]$.
 - 7: **end for**
 - 8: Get the total loss for the t -token prediction as $\mathcal{L} = \frac{1}{t} \sum_{i=0}^{t-1} \ell_i$
-

length (in tokens) a , choose a target length t (in tokens), and a random string of t tokens as the target sequence T . We then use the Adam optimizer (Kingma and Ba, 2014) and the gradient of the loss specified in Figure 8 with respect to the attack vector, P , as

$$g = \frac{\partial \mathcal{L}(S, T, P)}{\partial P}. \tag{8}$$

Using the gradient directly is the same technique as used in the original Szegedy et al. (2013), however, small modifications, such as keeping just the gradient signs (Goodfellow et al., 2015) are readily available as well.

Decreasing the language modeling loss \mathcal{L} by changing the activation attack P translates into making the model more likely to predict the desired t -token continuation T after the context S by changing the activations of the first a tokens. We stop the experiment either 1) after a predetermined number of optimization steps, or 2) once the t -token target continuation T is the argmax sampled continuation of the context S , by which we define a successful attack.

3.4 Estimating the attack multiplier κ

Our goal is to empirically measure under what conditions adversarial examples are *generally* possible and easy to find. We use random tokens sampled uniformly both for the context S as well as the targets T to ensure fairness. For a fixed attack length a and a context size $s \geq a$, we sweep over target lengths t in a range from 1 to typically over 1000 in logarithmic increments. For each fixed (a, t) , we repeat an experiment where we generate random context tokens S , and random target tokens T , and run the optimization at learning rate 10^{-1} for 300 steps. The success of each run is the fraction of the continuation tokens T that are correctly predicted using argmax as the sampling method. This gives us, for a specific context length s , attack length a , and a target length t an estimate of the attack success probability $p(a, t)$. The plot of this probability can be seen in e.g. Figure 5a and Table 1 refers to the appropriate figure for each model. The $p(a, t)$ are our main experimental result and we empirically estimate them for a range of language models and context sizes s .

For short target token sequences, the probability of a successful attack is high, and for long target sequences, the attacker is not able to control the model output sufficiently, resulting in a low probability. To $p(a, t)$ we fit a sigmoid curve of the form

$$\sigma(t, \alpha, \beta) = 1 - (1 + \exp(-\alpha(\log(t) - \log(t_{\max}))))^{-1}, \quad (9)$$

and read-off the best fit value of t_{\max} , for which the success rate of the attack of length a falls to 50%. In our scaling laws, we work with these values of t_{\max} , however, the 50% threshold is arbitrary and can be chosen differently.

Empirically, the read-off value of the 50% attack success threshold t_{\max} depends linearly on the number of attack tokens a whose activations the attacker can modify. The linearity of the relationship can be seen in e.g. Figure 7. As described in Section 2, we call the constant of proportionality the *attack multiplier* κ , and it relates the attack and target lengths as $t_{\max} = \kappa a$.

We empirically observe that the attack multiplier κ depends linearly on the dimension of the model activations used even across different models. We also theoretically expect this in Section 2. The *attack resistance* χ , defined in Equation 5, can be calculated from the estimated attack multiplier κ with the knowledge of the model activation numerical precision p (in our case 16 bits in all cases), activation dimension d (varied from 512 to 2560), and vocabulary size V (around 50,000 for all experiments) as

$$\chi = \frac{dp}{\kappa \log_2 V}. \quad (10)$$

We provide these estimates in Table 1.

In Fort (2023) adversarial *multi-attacks* are defined and described. They are attacks in which a single adversarial perturbation P is able to convert n inputs into n attacker-chosen classes. We ran a similar experiment where a single adversarial perturbation P can make the context S_1 complete as T_1 , S_2 as T_2 , and all the way to S_n to T_n . This effectively decreases the attack length a by a factor of n , or equivalently increases the target length by the same factor, as discussed on dimensional grounds in Section 2. Practically, we accumulate gradients over the n (S, T) pairs before taking an optimization step on P . We study multi-attacks from $n = 1$ (the standard attack) to $n = 8$.

Another modification described in Section 2 is to use only a random, fixed fraction f of the dimensions of the activation vector P . Its effect is to change the effective attack length from a to fa , and we choose the mask uniformly at random.

3.5 Token substitution attacks

To compare the attack on activations to the more standard attack on the input tokens themselves, we used a greedy, token-by-token, exhaustive search over all attack tokens a at the beginning of the context S . For a randomly chosen context S , an attack length $a \leq |S|$, and a randomly chosen sequence of target tokens T , we followed the algorithm in Figure 12 to find the first a tokens of the context that maximize the probability of the continuation T . By greedily searching over all V possible tokens, each attack token at a time, we can

Algorithm 2 Greedy, exhaustive token attack towards a t -token target sequence

- 1: **Given** tokens of context S of length $s = |S|$, attack length a ($a \leq s$), target tokens T of length t , and a vocabulary of size V
 - 2: The current context sequence starts at $S' = S$
 - 3: **for** $i = 0$ **to** $a - 1$ **do**
 - 4: {Looping over attack tokens}
 - 5: **for** $\tau = 0$ **to** $V - 1$ **do**
 - 6: {Looping over all possible single tokens}
 - 7: $S'[i] = \tau$ {Trying the new token}
 - 8: Calculate the language modeling loss \mathcal{L}_τ for the target continuation T after the context S' . If it is lower than the best so far, keep the $\tau_{\text{best}} = \tau$.
 - 9: **end for**
 - 10: Update the i^{th} attack token to the best, greedily, as $S'[i] = \tau_{\text{best}}$ {Greedy sampling token by token. Each token is searched exhaustively.}
 - 11: **end for**
 - 12: If the newly updated context S' produces the continuation T as the result, the attack is successful.
-

guarantee convergence in aV steps. We repeat this experiment over different values of the attack length a , and random contexts S and targets T of length $t = |T|$, obtaining a similar $p_{\text{token}}(a, t)$ curve as for the activation attacks. We fit the Eq. 9 sigmoid to it, extracting an equivalent attack multiplier κ_{token} , characterizing how many tokens on the output can a single token on the input influence (the result is, unlike for the activation attacks, much smaller than 1, of course).

3.6 Attack and target separation within the context

The further the attack is from the target, the less effective it might be. We therefore experiment with different sizes of the context S that separate the first a token activations of the attack from the target tokens after S . We estimate an attack multiplier for each s , getting a $\kappa(s)$ curve that we show in Figure 8. The attack multiplier κ looks constant up to a point (around 100 tokens of context) and then decreases linearly in $\log(s)$. We therefore fit a simple function of this form to our data in Figure 8.

4 Results and Discussion

We have been using the EleutherAI/pythia series of Large Language Models (Biderman et al., 2023) based on the GPT-NeoX library (Andonian et al., 2021; Black et al., 2022) from Hugging Face¹. A second suite of models we used is the microsoft/phi-1² (Li et al., 2023). Finally, we used a single checkpoint of roneneldan/TinyStories³ presented in Eldan and Li (2023). We ran our experiments on a single A100 GPU on a Google Colab.

For finding the adversarial attacks on activations, we used the Adam optimizer (Kingma and Ba, 2017) at a learning rate of 10^{-1} for 300 optimization steps, unless explicitly stated otherwise. Our activations

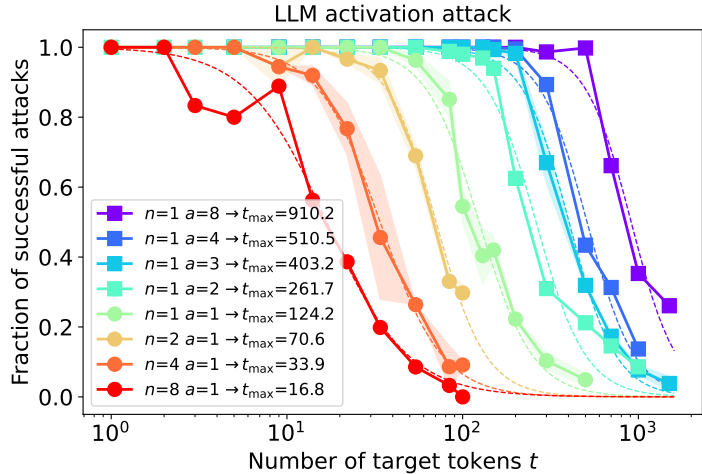
¹<https://huggingface.co/EleutherAI/pythia-70m>

²<https://huggingface.co/microsoft/phi-1>

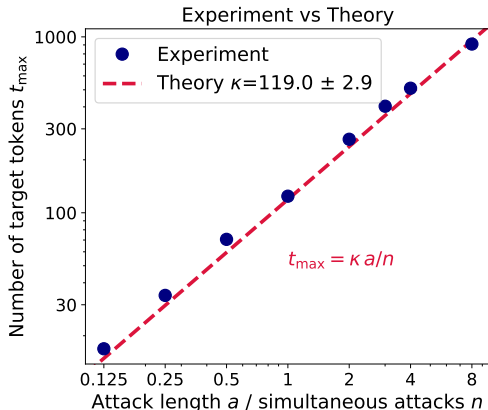
³<https://huggingface.co/datasets/roneneldan/TinyStories>

were all in the `float16` format, and the model vocabulary sizes were all very close to $V \approx 50,000$. For the input context as well as our (multi-)token target sequences, we sampled random tokens from the vocabulary uniformly. When using only a subset of the activations, as described in Section 3, we choose the dimensions at random uniformly.

4.1 Attacks on activations



(a) Fraction of successfully predicted target tokens as function of the number of target tokens t for different numbers of simultaneous attacks n and the length of the attack a .



(b) The maximum number of successfully converted attack tokens t_{\max} as a function of the ratio between the attack length a divided by the number of simultaneous attacks n . The linear dependence fits our theory well.

Figure 5: A summary of adversarial attacks on activations of EleutherAI/pythia-1.4b-v0. Only experiments varying the attack length a (in tokens whose activations the attacker controls) and the multiplicity of context and target pairs the attack has to succeed on, n , are shown. The estimated attack multiplier is $\kappa = 119.0 \pm 2.9$ which means that controlling a single token worth of activations on the input allows the attacker to determine ≈ 119 tokens on the output.

We ran adversarial attacks on model activations right after the embedding layer for a suite of models, a range of attack lengths a , target token lengths t , and multiple repetitions of each experimental setup (with different random tokens of context S and target T each time), obtaining an empirical probability of attack success $p(a, t)$ for each setting. For multiple repetitions, we also had a standard deviation of p at each set of (a, t) values. To get to lower effective values of a and therefore weaker attacks, we use the multi-attack strategy described in Section 3 and in Fort (2023), designing the same adversarial attack for up to $n = 8$ sequences and targets at once.

Figure 5 shows an example of the results of our experiments on EleutherAI/pythia-1.4b-v0, a 1.4B model with activation dimension $d = 2048$. In Figure 5a the success rates of attacks p for different values of attack length a (in tokens whose activations the attacker controls), target length t (in predicted output tokens), and the attack multiplicity n (how many attacks at once the same perturbation P has to succeed on simultaneously). The higher the attack length a , the more powerful the attack and the longer the target sequence t that can be controlled by it. We fit a sigmoid from Eq. 9 to each curve to estimate the maximum target sequence length, t_{\max} , at which the success rate of the attack drops to 50% (an arbitrary value).

In Figure 5b, we plot these t_{\max} maximum target lengths as a function of the attack strength a . Since the multi-attack n allows us to effectively go below $a = 1$, we actually plot a/n , the effective attack strength. Fitting our scaling law from Eq. 2 justified on geometric and dimensional grounds in Section 2, we estimate the attack multiplier for EleutherAI/pythia-1.4b-v0 to be $\kappa = 119.2 \pm 2.9$, implying that by controlling a single

Model	Curves	Size	Dimension d	$ V $	Attack multiplier κ	Per dim multiplier d/κ	Attack resistance χ
pythia-70m	Fig 10	70M	512	50304	24.2 ± 0.8	21.2 ± 0.7	21.7 ± 0.7
pythia-160m	Fig 11	160M	768	50304	36.2 ± 2.0	21.2 ± 1.2	21.7 ± 1.2
pythia-410m-deduped	Fig 12	410M	1024	50304	70.1 ± 2.3	14.6 ± 0.5	15.0 ± 0.5
pythia-1.4b-v0	Fig 5	1.4B	2048	50304	128.4 ± 3.7	16.0 ± 0.5	16.3 ± 0.5
pythia-2.8b-v0	Fig 13	2.8B	2560	50304	104.9 ± 2.2	24.4 ± 0.5	25.0 ± 0.5
Phi-1	Fig 14	1.3B	2048	50120	42.8 ± 2.3	47.9 ± 2.6	49.0 ± 2.6
Phi-1.5	Fig 15	1.3B	2048	50120	78.4 ± 5.1	26.1 ± 1.7	26.8 ± 1.7
TinyStories-33M	Fig 16	33M	768	50257	27.2 ± 2.2	28.2 ± 2.3	28.9 ± 2.3

Table 1: A summary of attack multipliers κ estimated from experiments for activation adversarial attacks for various language models. d/κ is the number of dimensions of an activation needed to control a single output token, while χ is the attack resistance (defined in Theory 10) which corresponds to the number of typical bits on the input the attacker has to control in order to have a single bit of control on the output. The pythia-* models are from EleutherAI, Phi-* from Microsoft and TinyStories-* from roneneldan.

token worth of activations at the beginning of a context, the attacker can determine ≈ 119 tokens exactly on the output. The results shown in Figure 5 only include experiments with attack lengths $a = 1, 2, 3, 4, 8$ and $n = 1$, and attack length $a = 1$ with a varying $n = 1, 2, 4, 8$. Varying n allows us to go to "sub"-token levels of attack strength.

4.2 Using only a fraction of dimensions

Another way of modifying the attack strength is to choose only a fraction f of the activation dimensions the attacker controls. Our geometric theory described in Section 2 suggests that the effective attack strength depends on the product of the attack length a , the fraction f and of the attack multiplicity as $1/n$. Therefore we should be able to vary (f, a, n) as we wish and the attack strength should only depend on fa/n . In Figure 6 we can see a comparison of experiments at the same attack strength performed at different combinations of a , n and f . In total 12 experimental setups are shown: 1) $n = 1$ and $f = 1$, while varying $a = 1, 2, 3, 4, 8$, 2) $a = 1$, $f = 1$, and $n = 2, 4, 8$, 3) $n = 1$, $a = 1$, and $f = 1/8, 1/4, 1/2$, and 4) $n = 8$, $a = 8$, and $f = 1/2$. All of these lie on the theoretical predicted scaling law in Eq. 4 as $t_{\max} = \kappa fa/n$. The estimated attack multiplier $\kappa = 128.4 \pm 3.7$ is well within 2σ of the estimate using the varying a and n alone in Figure 5.

4.3 Model comparison

For a number of different models, we show the scaling laws for attack strength a (in tokens whose activations the attacker can control) vs target length t (in tokens) in Figure 7. For each model, we estimate the attack multiplier κ (the number of target tokens the attacker can control with a 50% success rate by attacking the activation of a single token on the input), and compute their attack resistance χ , as defined in Eq. 10, corresponding to the number of bits the attacker needs to control on the input in order to control a single bit on the output. We summarize these results in Table 1.

An interesting observation is that while the model trainable parameter counts span two orders of magnitude (from 33M to 2.8B), and their activation dimensions range from 512 to 2560, the resulting relative attack multipliers κ/d , and the attack resistances χ stay surprisingly constant.

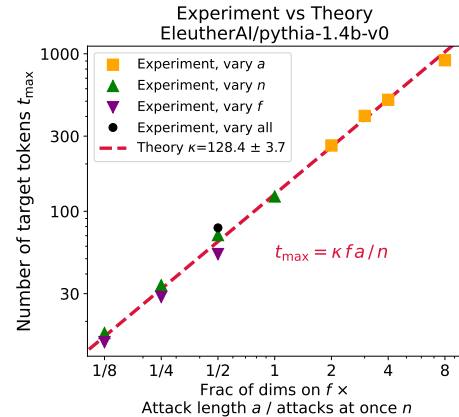


Figure 6: A scaling plot showing successful attacks on Pythia-1.4B for different attack lengths a , fraction of dimensions f , and attack multiplicities n .

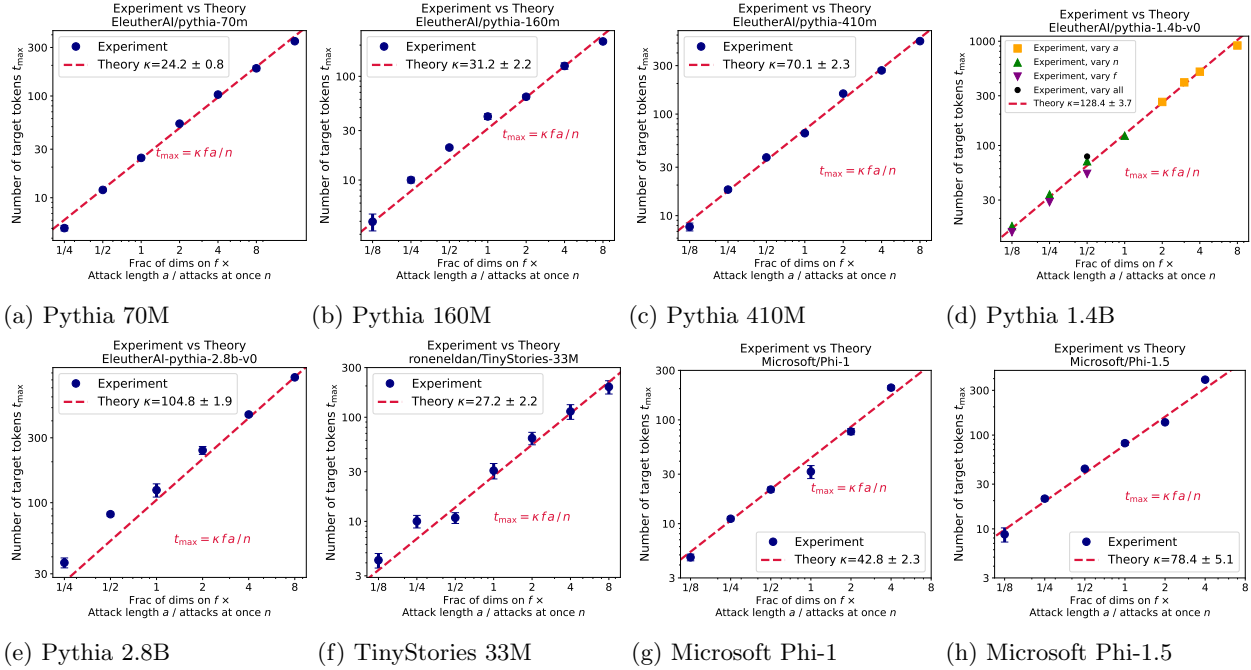


Figure 7: A summary of experiments to determine scaling laws for different models and to read off their attack multiplier κ . The individual plots show the results of fits to the success rate of attacking a language model by modifying its activations towards the target of generating t tokens as a function of a token activations of an attack. Our theory predicts a linear dependence in each plot, while the slope κ (the attack multiplier) is a model-specific constant.

This is supporting evidence for our geometric view of the adversarial attack theory presented in Section 2. The conclusion is that for the EleutherAI/pythia-* model family, we need between ≈ 15 and ≈ 25 bits controlled by the attacker on the model input (the activations of the context) in order to control in detail the outcome of a single bit on the model output (the argmax predictions from the model). In an ideal scenario, where a single dimension / bit on the input could influence a single dimension / bit on the output, each activation dimension would be able to control a single token on the output since the model activations are typically 16 bits and to determine a single token we also need $\log_2(V) \approx 16$ bits. However, since we need $\chi > 1$ bits on the input to affect one on the output, this means that we need χ activation dimensions to force the model to predict a token exactly as we want. This is still a remarkable strong level of control, albeit weaker than one might naively expect.

4.4 Context separating the attack and the target tokens

In our experiments, we attack the activations of the first a tokens of the context of length s ($a \leq s$) in order to make the model predict an arbitrary t -token sequence of tokens as its argmax continuation. In our most standard experiments $a = s$, which means that the attacker controls the activations of the full context which

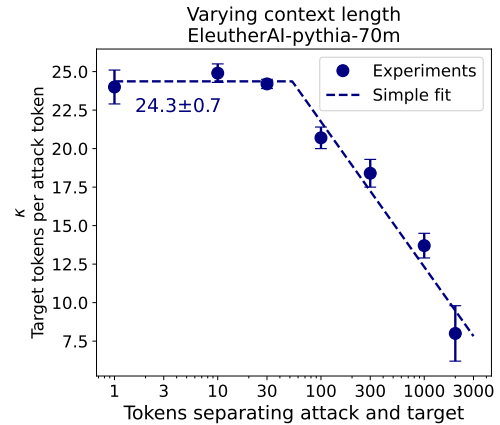


Figure 8: The effect of tokens separating the attack and the target. Up to 100 tokens of separation, the attack multiplier (strength) does not diminish. After that it drops logarithmically up to the context window size.

is of exactly the same length as the attack. These are the experiments in Figure 5, summary Figure 7 and the summary Table 1. To see the effect of having context tokens separating the attack from the target tokens, we ran an experiment with a fixed model `EleutherAI/pythia-70m` and read off the attack multiplier κ for each context length s in a logarithmically spaced range from 1 to 2000 (almost the full context window size). Estimating each $\kappa(s)$ involved exploring a range of target lengths a and attack multipliers n , each in turn being a 300 step optimization of the attack, as described in Section 4. The results are shown in Figure 8. We see that for up to 100 tokens of separation between the attack and the target tokens, there is no visible drop in the attack multiplier κ . In other words, the attack is equally effective at forcing token predictions immediately after its own tokens or 100 tokens down the line. After the context length of ≈ 100 we see a linear drop in $\kappa(s)$ with a log of the context length. At 2000 tokens of random context separating the attack and the target, we still see $\kappa \approx 8$, i.e. a single token’s activations on the input controlling 8 tokens on the output.

4.5 Replacing tokens directly

To compare the effect of attacking the activation vectors and attacking the input tokens directly by replacing them, we ran experiments on the `EleutherAI/pythia-70m` model. For a randomly chosen context of $s = 40$ tokens and randomly chosen t -token target tokens ($t = 1, 2, 4$ in our experiments) we greedily and per-token-exhaustively search over the replacements of the first a tokens of the context in order to make the model predict the desired t -token sequence as a continuation. The method is described in Section 3 in detail.

Unlike for activation attacks, the token replacement attack needs more than one token on the input to influence a single token on the output. The detailed curves showing the attack success rate $p(a, t)$ as a function of the attack length a (the number of tokens the attacker can replace by other tokens) and the target length t are shown in Figure 9, together with Eq. 9 fits to them to extract the a_{\min} , the minimum attack length to force the prediction of a t -token sequence. For $t = 1$, we get $a_{\min} = 11.7 \pm 0.2$, while for $t = 2$ $a_{\min} = 16.7 \pm 0.2$ and for $t = 4$ $a_{\min} = 33.4 \pm 1.1$. Extracting the attack multiplier $\kappa_{\text{token}} = t/a_{\min}$, we get 0.085 ± 0.001 , 0.120 ± 0.002 and 0.120 ± 0.004 . Averaging the three estimates while weighting them using the squares of their errors, we get $\kappa_{\text{token}} \approx 0.12$. That means that we need $1/\kappa_{\text{token}} \approx 8$ tokens to control on the input in order to force the prediction of a single token on the output by token replacement (compared to ≈ 0.04 tokens worth for the activations attack in Table 1).

Controlling tokens instead of activations offers the attacker a greatly diminished dimensionality of the space they can realize the attack in. In Section 2, we discuss the comparison between the dimensionality of the token attack ($\log_2(V)a$ bits of control for an a token attack), compared to the activations attack (adp bits of control for a precision $p = 16$ and $d = 512$ for `EleutherAI/pythia-70m` in particular). Our geometric theory predicts that their attack multipliers should be in the same ratio as the dimensions of the spaces the attacker controls. In this particular case, the theory predicts $\kappa_{\text{token}}/\kappa = \log_2(V)/(dp) \approx 2 \times 10^{-3}$. The actual experimentally estimated values give us $\kappa_{\text{token}}/\kappa \approx 5 \times 10^{-3}$. Given how simple our theory is and how different the activation vs token attacks are, we find the empirical result to match the prediction surprisingly well (it is better than an order of magnitude match).

If we calculated the attack resistance χ_{token} for the token attack, we would get directly $\chi_{\text{token}} = 1/\kappa_{\text{token}} =$

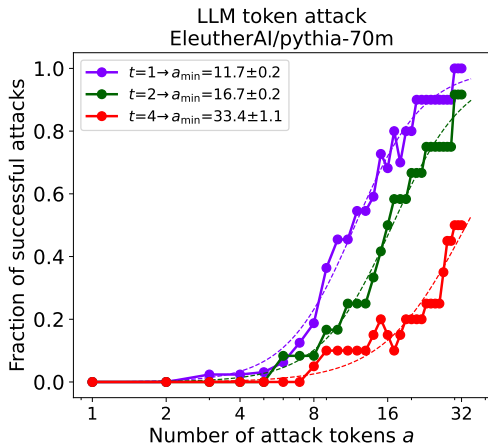


Figure 9: Greedy search over all attack tokens to get specific target completions. We use the first a tokens (x-axis) of the context and for each of them, starting at the first, choose the token among the full vocabulary that minimizes the loss for the t token completion of the given context. In general, ≈ 8 tokens worth of attack are needed to force a single particular token of a response.

Model	Attack type	Curves	Size	Dimension d	$ V $	Attack multiplier κ	Attack resistance χ
pythia-70m	Tokens	Fig 9	70M	512	50304	0.12	8.3
	Activations	Fig 10	70M	512	50304	24.2 ± 0.8	21.7 ± 0.7

Table 2: Comparing activation attacks and token attacks on EleutherAI/pythia-70m. The activation attack has a much higher attack multiplier $\kappa = 24.2 \pm 0.8$ compared to the one for token attack of $\kappa_{\text{token}} \approx 0.12$. While a single token’s activation can therefore determine > 20 output tokens, the attacker needs > 8 input tokens to control a single one by token replacement. Our geometric theory predicts that this is the consequence of the lower dimension of the token space compared to the activation space. If that were the case, the attack resistance χ , measuring how many bits of control on the input are needed to determine a bit on the output, should be the same for both attack types. Our experiments show that they are a factor of $2.6\times$ from each other, which is a close match given the simplicity of our theory and the vastly different nature of the two attack types.

8.3. That means that ≈ 8 bits of control are needed by the attacker on the input to control a single bit of the model predictions. This shows that the token attack is much more efficient than the activations attack ($\chi \approx 22$ for this model), which makes sense given that the model was trained to predict tokens after receiving tokens on the input rather than arbitrary activation vectors not corresponding to anything seen during training.

5 Conclusion

Our research presents a detailed empirical investigation of adversarial attacks on language model activations, demonstrating a significant vulnerability that exists within their structure. By targeting a small amount of language model activations that can be hidden deep within the context window and well separated from their intended effect, we have shown that it is possible for an attacker to precisely control up to $\mathcal{O}(100)$ subsequent predicted tokens down to the specific token IDs being sampled. The general method is illustrated in Figure 1.

We empirically measure the amount of target tokens t_{max} an attacker can control by modifying the activations of the first a tokens in the context window, and find a simple scaling law of the form

$$t_{\text{max}}(a) = \kappa a, \tag{11}$$

where we call the model-specific constant of proportionality κ the *attack multiplier*. We conduct a range of experiments on models from 33M to 2.8B parameters and measure their attack multipliers κ , summarized in Figure 7 and Table 1.

We connect these to a simple geometric theory that attributes adversarial vulnerability to the mismatch between the dimension of the input space the attacker controls and the output space the attacker would like to influence. This theory predicts a linear dependence between the critical input and output space dimensions for which adversarial attacks stop being possible, which is what we see empirically in Figure 7. By using language models as a controllable test-bed for studying regimes of various input dimensions (controlled by the attack length a) and output dimension (controlled by the target sequence length t), we were able to explore parameter ranges that were not previously accessible in computer vision experiments where the study of adversarial examples was historically rooted.

We find that empirically, the attack multiplier κ seems to depend linearly on the model activation dimension d rather than the model parameters, as predicted by our geometrical theory. κ/d , as shown in Table 1, is surprisingly constant between 16.0 ± 0.5 and 24.4 ± 0.5 for the EleutherAI/pythia model suite spanning model sizes from 70M to 2.8B parameters.

Comparing dimensions of the input and output spaces in bits, we define attack resistance, χ , as the amount of bits an attacker has to control on the input in order to influence a single bit on the output, and

theoretically relating this to the model activation (also called residual stream) dimension d , vocabulary size V , and floating point precision p ($p = 16$ for `float16` used) as

$$\chi = \frac{dp}{\kappa \log_2 V}. \tag{12}$$

We find that for the EleutherAI/pythia model suite, the attacker needs to control between 15 and 25 bits of the input space in order to control a single bit of the output space (the most naive theory would predict $\chi = 1$, each input dimension controlling an output dimension).

We compare the activation attacks to the more standard token substitution attacks in which the attacker can replace the first a tokens of the context in order to make the model predict a specific t -token sequence. In Figure 9 and Table 2 we summarize our results and show that despite the token attack being much weaker (on our 70M model) with an attack multiplier of $\kappa_{\text{token}} \approx 0.12$ (meaning that we need 8 tokens of input control to make the model predict a single output token) compared to the activation attack $\kappa = 24.2$, the two vastly different attack types have a very similar attack resistance χ when accounting for the vastly different dimensions of the input space of tokens and activations. The theoretically predicted $\kappa/\kappa_{\text{token}} = 2 \times 10^{-3}$ is surprisingly close to the empirically measured 5×10^{-3} despite the arguable simplicity of the theory. It seems that model input tokenization is in (some) meaningful sense a very powerful defense against adversarial attacks by vastly reducing the dimension of the space the attacker can control.

To make sure our findings are robust to a separation between the attack tokens and the target tokens, we experiment with adding up to $\mathcal{O}(1000)$ randomly sampled tokens between the attack and the target in Figure 8. We find that the attack strength essentially unaffected up to 100 tokens of separation with a logarithmic decline after. However, even a full context of separation gives a high degree of control of the very first token activation over the next-token prediction.

Attacking activations might seem impractical since the majority of language models, especially the commercial ones, allow users to interact with them only via token inputs. However, an increasing attack surface due to multi-modal models, where other modalities are added to the activations directly, as well as some retrieval models, where retrieved documents are mixed-in likewise as activations rather than tokens, directly justify the practical relevance of this paper.

Some additional directions that would be great to explore are: 1) attacking activations beyond the first layer (we tested this and it works equally well), 2) using natural language strings for contexts and targets rather than random samples from the vocabulary (our initial experiments did not suggest a big difference), and 3) size-limited adversarial perturbations, as is usual in computer vision, where the amount an image can be perturbed for an attack to count is often limited by the L_∞ or L_2 norms of the perturbation.

In conclusion, our research underscores a critical vulnerability in LLMs to adversarial attacks on activations. This vulnerability opens up new avenues for both defensive strategies against such attacks and a deeper understanding of the architectural strengths and weaknesses of language models. As language models continue to be integrated into increasingly critical applications, addressing these vulnerabilities becomes essential for ensuring the safety and reliability of AI systems. In addition, a simple geometric theory that attributes adversarial vulnerabilities to the dimensional mismatch between the space of inputs and the space of outputs seems to be supported by our results. Our observed, linear scaling laws between the input dimension and its resulting control over the output is a clear signal, and so is the surprising similarity between attacking tokens and activations in terms of their strength, when their dimensionalities are properly accounted for. The language model setup also proved to be an excellent controllable test-bed for understanding adversarial attacks in input-output dimensionality regimes that are inaccessible in computer vision setups.

References

- Christian Szegedy, Wojciech Zaremba, Ilya Sutskever, Joan Bruna, Dumitru Erhan, Ian Goodfellow, and Rob Fergus. Intriguing properties of neural networks, 2013.
- Nelson Elhage, Neel Nanda, Catherine Olsson, Tom Henighan, Nicholas Joseph, Ben Mann, Amanda Askell, Yuntao Bai, Anna Chen, Tom Conerly, Nova DasSarma, Dawn Drain, Deep Ganguli, Zac Hatfield-Dodds, Danny Hernandez, Andy Jones, Jackson Kernion, Liane Lovitt, Kamal Ndousse, Dario Amodei, Tom Brown, Jack Clark, Jared Kaplan, Sam McCandlish, and Chris Olah. A mathematical framework for transformer circuits. *Transformer Circuits Thread*, 2021. <https://transformer-circuits.pub/2021/framework/index.html>.
- Ian J. Goodfellow, Jonathon Shlens, and Christian Szegedy. Explaining and harnessing adversarial examples, 2015.
- Martin Abadi, Andy Chu, Ian Goodfellow, H. Brendan McMahan, Ilya Mironov, Kunal Talwar, and Li Zhang. Deep learning with differential privacy. In *Proceedings of the 2016 ACM SIGSAC Conference on Computer and Communications Security, CCS'16*. ACM, October 2016. doi: 10.1145/2976749.2978318. URL <http://dx.doi.org/10.1145/2976749.2978318>.
- Andrew Ilyas, Shibani Santurkar, Dimitris Tsipras, Logan Engstrom, Brandon Tran, and Aleksander Madry. Adversarial examples are not bugs, they are features, 2019.
- Sebastian Borgeaud, Arthur Mensch, Jordan Hoffmann, Trevor Cai, Eliza Rutherford, Katie Millican, George van den Driessche, Jean-Baptiste Lespiau, Bogdan Damoc, Aidan Clark, Diego de Las Casas, Aurelia Guy, Jacob Menick, Roman Ring, Tom Hennigan, Saffron Huang, Loren Maggiore, Chris Jones, Albin Cassirer, Andy Brock, Michela Paganini, Geoffrey Irving, Oriol Vinyals, Simon Osindero, Karen Simonyan, Jack W. Rae, Erich Elsen, and Laurent Sifre. Improving language models by retrieving from trillions of tokens, 2022.
- Jean-Baptiste Alayrac, Jeff Donahue, Pauline Luc, Antoine Miech, Iain Barr, Yana Hasson, Karel Lenc, Arthur Mensch, Katie Millican, Malcolm Reynolds, Roman Ring, Eliza Rutherford, Serkan Cabi, Tengda Han, Zhitao Gong, Sina Samangooei, Marianne Monteiro, Jacob Menick, Sebastian Borgeaud, Andrew Brock, Aida Nematzadeh, Sahand Sharifzadeh, Mikolaj Binkowski, Ricardo Barreira, Oriol Vinyals, Andrew Zisserman, and Karen Simonyan. Flamingo: a visual language model for few-shot learning, 2022.
- Edoardo DeBenedetti, Giorgio Severi, Nicholas Carlini, Christopher A. Choquette-Choo, Matthew Jagielski, Milad Nasr, Eric Wallace, and Florian Tramèr. Privacy side channels in machine learning systems, 2023.
- Yuntao Bai, Andy Jones, Kamal Ndousse, Amanda Askell, Anna Chen, Nova DasSarma, Dawn Drain, Stanislav Fort, Deep Ganguli, Tom Henighan, Nicholas Joseph, Saurav Kadavath, Jackson Kernion, Tom Conerly, Sheer El-Showk, Nelson Elhage, Zac Hatfield-Dodds, Danny Hernandez, Tristan Hume, Scott Johnston, Shauna Kravec, Liane Lovitt, Neel Nanda, Catherine Olsson, Dario Amodei, Tom Brown, Jack Clark, Sam McCandlish, Chris Olah, Ben Mann, and Jared Kaplan. Training a helpful and harmless assistant with reinforcement learning from human feedback, 2022.
- Stephen Casper, Xander Davies, Claudia Shi, Thomas Krendl Gilbert, Jérémy Scheurer, Javier Rando, Rachel Freedman, Tomasz Korbak, David Lindner, Pedro Freire, Tony Wang, Samuel Marks, Charbel-Raphaël Segerie, Micah Carroll, Andi Peng, Phillip Christoffersen, Mehul Damani, Stewart Slocum, Usman Anwar, Anand Siththaranjan, Max Nadeau, Eric J. Michaud, Jacob Pfau, Dmitrii Krasheninnikov, Xin Chen, Lauro Langosco, Peter Hase, Erdem Bıyık, Anca Dragan, David Krueger, Dorsa Sadigh, and Dylan Hadfield-Menell. Open problems and fundamental limitations of reinforcement learning from human feedback, 2023.
- Andy Zou, Long Phan, Sarah Chen, James Campbell, Phillip Guo, Richard Ren, Alexander Pan, Xuwang Yin, Mantas Mazeika, Ann-Kathrin Dombrowski, Shashwat Goel, Nathaniel Li, Michael J. Byun, Zifan

- Wang, Alex Mallen, Steven Basart, Sanmi Koyejo, Dawn Song, Matt Fredrikson, J. Zico Kolter, and Dan Hendrycks. Representation engineering: A top-down approach to ai transparency, 2023a.
- Jared Kaplan, Sam McCandlish, Tom Henighan, Tom B. Brown, Benjamin Chess, Rewon Child, Scott Gray, Alec Radford, Jeffrey Wu, and Dario Amodei. Scaling laws for neural language models, 2020.
- Jordan Hoffmann, Sebastian Borgeaud, Arthur Mensch, Elena Buchatskaya, Trevor Cai, Eliza Rutherford, Diego de Las Casas, Lisa Anne Hendricks, Johannes Welbl, Aidan Clark, Tom Hennigan, Eric Noland, Katie Millican, George van den Driessche, Bogdan Damoc, Aurelia Guy, Simon Osindero, Karen Simonyan, Erich Elsen, Jack W. Rae, Oriol Vinyals, and Laurent Sifre. Training compute-optimal large language models, 2022.
- Elias Frantar, Carlos Riquelme, Neil Houlsby, Dan Alistarh, and Utku Evci. Scaling laws for sparsely-connected foundation models, 2023.
- Stanislav Fort, Jie Ren, and Balaji Lakshminarayanan. Exploring the limits of out-of-distribution detection. *arXiv preprint arXiv:2106.03004*, 2021.
- Suzana Herculano-Houzel. The remarkable, yet not extraordinary, human brain as a scaled-up primate brain and its associated cost. *Proceedings of the National Academy of Sciences*, 109(supplement_1):10661–10668, 2012. doi: 10.1073/pnas.1201895109. URL <https://www.pnas.org/doi/abs/10.1073/pnas.1201895109>.
- Can Kabadayi, Lucy A Taylor, Auguste MP von Bayern, and Mathias Osvath. Ravens, new caledonian crows and jackdaws parallel great apes in motor self-regulation despite smaller brains. *Royal Society Open Science*, 3(4):160104, 2016.
- Alex Turner, Lisa Thiergart, David Udell, Gavin Leech, Ulisse Mini, and Monte MacDiarmid. Activation addition: Steering language models without optimization, 2023.
- Andy Zou, Zifan Wang, J. Zico Kolter, and Matt Fredrikson. Universal and transferable adversarial attacks on aligned language models, 2023b.
- Boxin Wang, Weixin Chen, Hengzhi Pei, Chulin Xie, Mintong Kang, Chenhui Zhang, Chejian Xu, Zidi Xiong, Ritik Dutta, Rylan Schaeffer, Sang T. Truong, Simran Arora, Mantas Mazeika, Dan Hendrycks, Zinan Lin, Yu Cheng, Sanmi Koyejo, Dawn Song, and Bo Li. Decodingtrust: A comprehensive assessment of trustworthiness in gpt models, 2023.
- Alec Radford, Jong Wook Kim, Chris Hallacy, Aditya Ramesh, Gabriel Goh, Sandhini Agarwal, Girish Sastry, Amanda Askell, Pamela Mishkin, Jack Clark, Gretchen Krueger, and Ilya Sutskever. Learning transferable visual models from natural language supervision, 2021.
- Stanislav Fort. Pixels still beat text: Attacking the openai clip model with text patches and adversarial pixel perturbations, March 2021a. URL https://stanislavfort.github.io/2021/03/05/OpenAI_CLIP_stickers_and_adversarial_examples.html.
- Stanislav Fort. Adversarial examples for the openai clip in its zero-shot classification regime and their semantic generalization, Jan 2021b. URL https://stanislavfort.github.io/2021/01/12/OpenAI_CLIP_adversarial_examples.html.
- Stanislav Fort. Multi-attacks: Many images + the same adversarial attack → many target labels, 2023.
- Tom Henighan, Shan Carter, Tristan Hume, Nelson Elhage, Robert Lasenby, Stanislav Fort, Nicholas Schiefer, and Christopher Olah. Superposition, memorization, and double descent. *Transformer Circuits Thread*, 2023.
- Alex Krizhevsky, Vinod Nair, and Geoffrey Hinton. Cifar-10 (canadian institute for advanced research). a. URL <http://www.cs.toronto.edu/~kriz/cifar.html>.

- Alex Krizhevsky, Vinod Nair, and Geoffrey Hinton. Cifar-100 (canadian institute for advanced research). b. URL <http://www.cs.toronto.edu/~kriz/cifar.html>.
- Jia Deng, Wei Dong, Richard Socher, Li-Jia Li, Kai Li, and Li Fei-Fei. Imagenet: A large-scale hierarchical image database. In *2009 IEEE conference on computer vision and pattern recognition*, pages 248–255. Ieee, 2009.
- Tal Ridnik, Emanuel Ben-Baruch, Asaf Noy, and Lihi Zelnik-Manor. Imagenet-21k pretraining for the masses, 2021.
- Stanislav Fort, Ekin Dogus Cubuk, Surya Ganguli, and Samuel S. Schoenholz. What does a deep neural network confidently perceive? the effective dimension of high certainty class manifolds and their low confidence boundaries, 2022.
- Diederik P Kingma and Jimmy Ba. Adam: A method for stochastic optimization. *arXiv preprint arXiv:1412.6980*, 2014.
- Stella Biderman, Hailey Schoelkopf, Quentin Anthony, Herbie Bradley, Kyle O’Brien, Eric Hallahan, Mohammad Aflah Khan, Shivanshu Purohit, USVSN Sai Prashanth, Edward Raff, Aviya Skowron, Lintang Sutawika, and Oskar van der Wal. Pythia: A suite for analyzing large language models across training and scaling, 2023.
- Alex Andonian, Quentin Anthony, Stella Biderman, Sid Black, Preetham Gali, Leo Gao, Eric Hallahan, Josh Levy-Kramer, Connor Leahy, Lucas Nestler, Kip Parker, Michael Pieler, Shivanshu Purohit, Tri Songz, Wang Phil, and Samuel Weinbach. GPT-NeoX: Large Scale Autoregressive Language Modeling in PyTorch, 8 2021. URL <https://www.github.com/eleutherai/gpt-neox>.
- Sid Black, Stella Biderman, Eric Hallahan, Quentin Anthony, Leo Gao, Laurence Golding, Horace He, Connor Leahy, Kyle McDonell, Jason Phang, Michael Pieler, USVSN Sai Prashanth, Shivanshu Purohit, Laria Reynolds, Jonathan Tow, Ben Wang, and Samuel Weinbach. GPT-NeoX-20B: An open-source autoregressive language model. In *Proceedings of the ACL Workshop on Challenges & Perspectives in Creating Large Language Models*, 2022. URL <https://arxiv.org/abs/2204.06745>.
- Yuanzhi Li, Sébastien Bubeck, Ronen Eldan, Allie Del Giorno, Suriya Gunasekar, and Yin Tat Lee. Textbooks are all you need ii: phi-1.5 technical report, 2023.
- Ronen Eldan and Yuanzhi Li. Tinstories: How small can language models be and still speak coherent english?, 2023.
- Diederik P. Kingma and Jimmy Ba. Adam: A method for stochastic optimization, 2017.

A Detailed attack success rate curves for different models

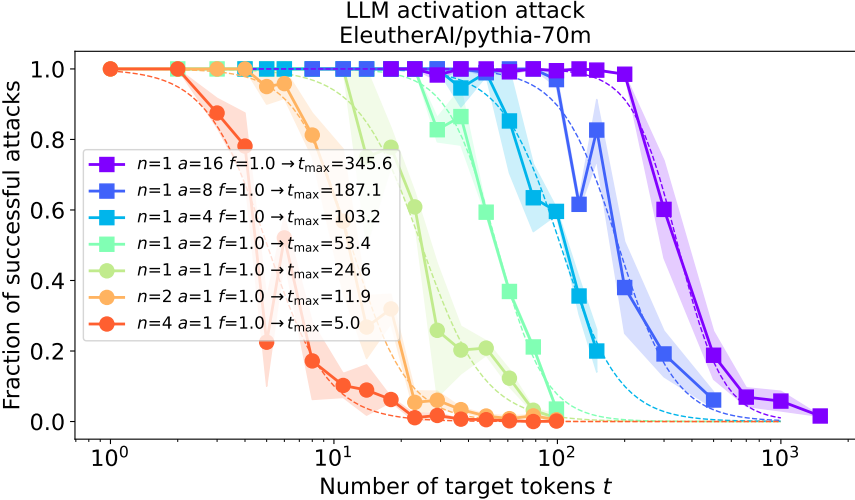


Figure 10: Fraction of successfully realized attack tokens as a function of the number of target tokens t for different numbers of simultaneous attacks n and the length of the attack a for EleutherAI/pythia-70m.

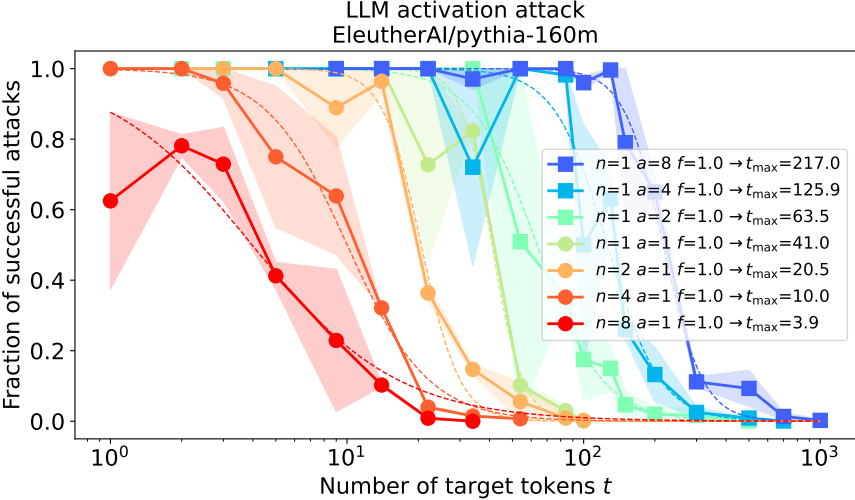


Figure 11: Fraction of successfully realized attack tokens as a function of the number of target tokens t for different numbers of simultaneous attacks n and the length of the attack a for EleutherAI/pythia-160m.

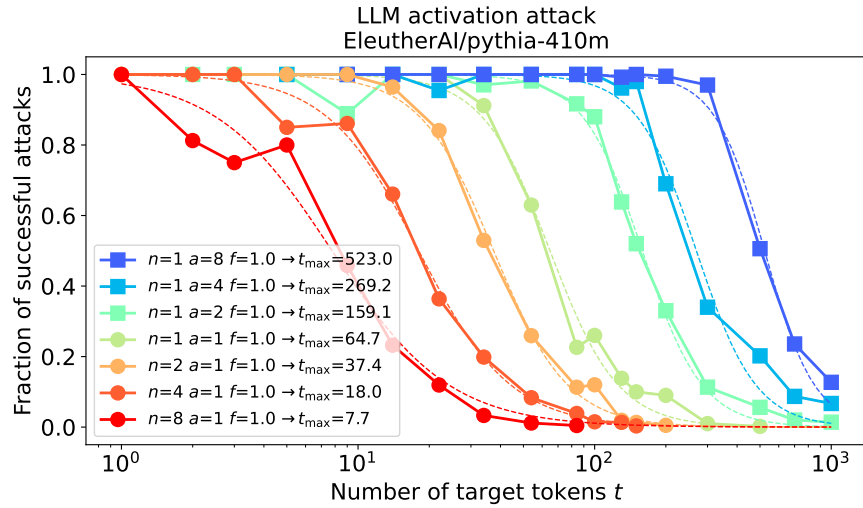


Figure 12: Fraction of successfully realized attack tokens as a function of the number of target tokens t for different numbers of simultaneous attacks n and the length of the attack a for EleutherAI/pythia-410m.

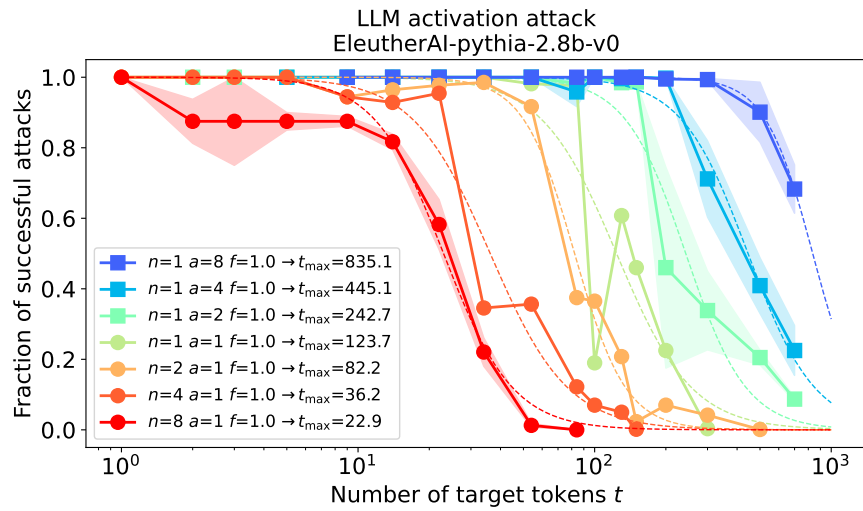


Figure 13: Fraction of successfully realized attack tokens as a function of the number of target tokens t for different numbers of simultaneous attacks n and the length of the attack a for EleutherAI/pythia-2.8b.

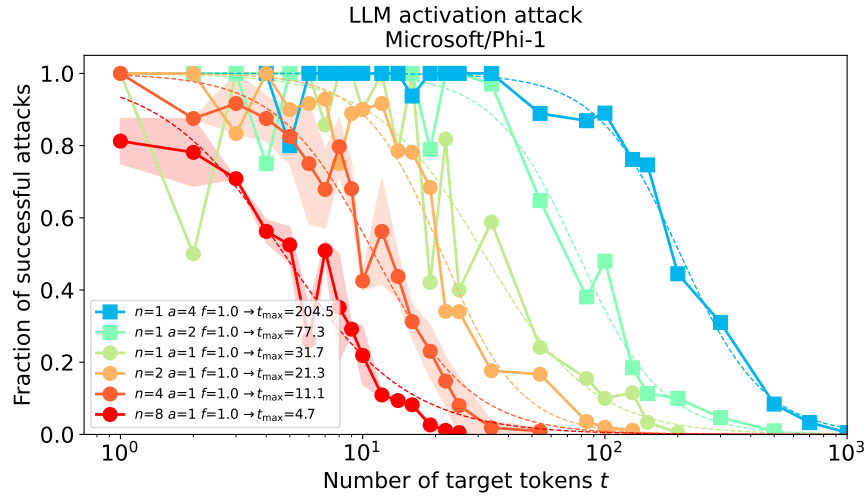


Figure 14: Fraction of successfully realized attack tokens as a function of the number of target tokens t for different numbers of simultaneous attacks n and the length of the attack a for Microsoft/Phi-1.

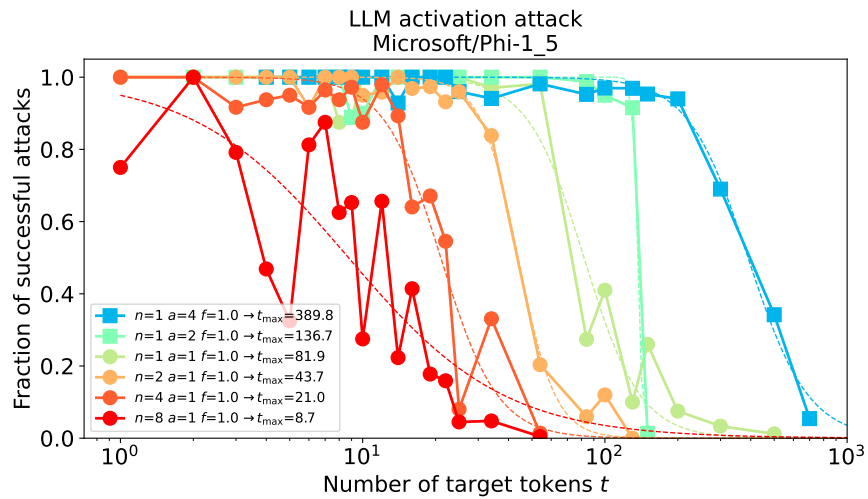


Figure 15: Fraction of successfully realized attack tokens as a function of the number of target tokens t for different numbers of simultaneous attacks n and the length of the attack a for Microsoft/Phi-1.5.

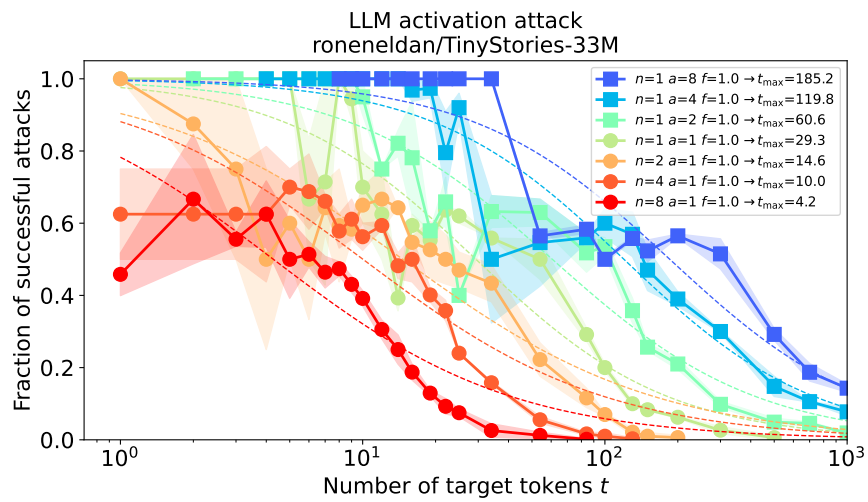


Figure 16: Fraction of successfully realized attack tokens as a function of the number of target tokens t for different numbers of simultaneous attacks n and the length of the attack a for ronenedan/TinyStories-33m.